

Homeostatic Synaptic Scaling Is Regulated by Protein SUMOylation^{*[5]}

Received for publication, February 27, 2012, and in revised form, April 27, 2012. Published, JBC Papers in Press, May 11, 2012, DOI 10.1074/jbc.M112.356337

Tim J. Craig^{‡1}, Nadia Jaafari^{‡1}, Milos M. Petrovic^{§¶}, Philip P. Rubin[‡], Jack R. Mellor[§], and Jeremy M. Henley^{‡2}

From the [‡]Medical Research Council Centre for Synaptic Plasticity, School of Biochemistry, and [§]School of Physiology and Pharmacology, University of Bristol, Bristol BS8 1TD, United Kingdom and the [¶]Institute of Medical Physiology, School of Medicine, University of Belgrade, 11000 Belgrade, Serbia

Background: SUMOylation regulates many cell pathways.

Results: Synaptic scaling elicited by suppression of neuronal activity decreases the deSUMOylating enzyme SENP1; overexpression of SENP1 prevents synaptic scaling.

Conclusion: SUMOylation is required for AMPA receptor trafficking underlying scaling, an important form of neuronal plasticity.

Significance: Regulation of synaptic dynamics and plasticity is fundamental to understanding brain function and dysfunction.

Homeostatic scaling allows neurons to alter synaptic transmission to compensate for changes in network activity. Here, we show that suppression of network activity with tetrodotoxin, which increases surface expression of AMPA receptors (AMPA receptors), dramatically reduces levels of the deSUMOylating (where SUMO is small ubiquitin-like modifier) enzyme SENP1, leading to a consequent increase in protein SUMOylation. Overexpression of the catalytic domain of SENP1 prevents this scaling effect, and we identify Arc as a SUMO substrate involved in the tetrodotoxin-induced increase in AMPAR surface expression. Thus, protein SUMOylation plays an important and previously unsuspected role in synaptic trafficking of AMPARs that underlies homeostatic scaling.

AMPA receptors (AMPA receptors)³ mediate most fast excitatory synaptic transmission in the central nervous system, and their regulated trafficking underlies NMDA receptor-dependent long-term potentiation and long-term depression (1). The changes in the efficacy of specific synapses that occur in long-term potentiation and long-term depression can lead, however, to destabilization of neuronal circuits. To counteract this, homeostatic scaling provides a compensatory mechanism that adjusts global synaptic properties to maintain differences in the relative strengths of synaptic inputs, which are necessary for information processing and storage (2, 3).

SUMOylation is the covalent conjugation of a small ubiquitin-like modifier (SUMO) protein to a lysine residue in target

proteins (4) at the consensus sequence ψ KX(D/E), where ψ is a large hydrophobic residue, e.g. valine. There are three SUMO paralogs, SUMO-1–SUMO-3, but SUMO-2 and SUMO-3 differ by only three amino acids. Despite being a covalent modification, most substrate proteins are rapidly deSUMOylated by SENP enzymes. There are six SENP enzymes (SENP1–SENP3 and SENP5–SENP7), and SENP1 has a broad specificity for SUMO-1 and SUMO-2/3 and acts in both their maturation and deconjugation (4).

The functional consequences of SUMO conjugation are diverse and, for many proteins, have not yet been fully established. Nonetheless, SUMOylation is integral to neuronal function and plays roles in synapse formation and regulation of axonal transport and neuronal excitability (5, 6). For example, SUMOylation of the kainate receptor subunit GluK2 by SUMO-1 is required for agonist-induced endocytosis of the receptor (7, 8). SUMOylation of other proteins has been shown to affect spine development and dynamics (9–11), presynaptic exocytosis (12), and neuronal excitability (13). Intriguingly, however, there have been no reports of SUMOylation influencing AMPAR localization or function.

The activity-induced immediate-early gene product Arc/Arg3.1 (Arc) is the most extensively characterized protein involved in synaptic scaling (2, 14). Arc mRNA undergoes activity-dependent dendritic transport and local protein synthesis. Arc levels are increased by sustained rises in synaptic activity and regulated by ubiquitination and proteasomal degradation. The neurodegenerative disease Angelman syndrome is suggested to be caused in part by defective Arc ubiquitination, leading to Arc accumulation and decreased synaptic AMPARs (15). The effect on AMPARs is specific, as overexpression of Arc enhances and knockdown reduces basal AMPAR endocytosis with no effects on NMDA receptor-dependent AMPAR long-term depression (16). Raised levels of Arc caused by increased neuronal activity promote AMPAR internalization via Arc interactions with endophilin-3 and dynamin-2, resulting in decreased AMPAR surface expression (14, 17). On the other hand, prolonged inhibition of synaptic activity decreases Arc levels, which leads to reduced endocytosis and increased

* This work was supported by the Medical Research Council and the European Research Council (to J. M. H.), the Biotechnology and Biological Sciences Research Council and the Wellcome Trust (to J. M. H. and J. R. M.), and a Marie Curie fellowship and a European Molecular Biology Organization short-term fellowship (to M. M. P.).

⌘ Author's Choice—Final version full access.

[5] This article contains supplemental Figs. S1 and S2.

¹ Both authors contributed equally to this work.

² To whom correspondence should be addressed: School of Biochemistry, Medical Sciences Bldg., University of Bristol, University Walk, Bristol BS8 1TD, UK. E-mail: j.m.henley@bristol.ac.uk.

³ The abbreviations used are: AMPAR, AMPA receptor; SUMO, small ubiquitin-like modifier; TTX, tetrodotoxin; EPSC, excitatory postsynaptic current.

Synaptic Scaling and SUMOylation

AMPA surface expression (14, 18). It has also been reported that Arc is involved in homeostatic plasticity at individual synapses, independent of neighboring synapses (19). Interestingly, SUMOylation has also been proposed as an important regulator of Arc function. Mutation of two consensus SUMOylation sites disrupts Arc localization in dendrites, which has been interpreted to suggest that Arc SUMOylation plays a role in structural changes required for some forms of long-term potentiation consolidation (20).

Here, we demonstrate that, consistent with previous reports, sustained blockade of synaptic activity with tetrodotoxin (TTX) increases AMPAR surface expression. In addition, however, TTX reduces the levels of SENP1, which in turn increases protein SUMOylation by SUMO-1. Overexpression of SENP1 prevents the TTX-induced increase in GluA1. We further show that SUMOylation of Arc is a key regulator of AMPAR trafficking in synaptic scaling.

EXPERIMENTAL PROCEDURES

Molecular Biology—The SENP1 catalytic domain (residues 351–644; SENP1(active)) and SENP1(C603S) were subcloned into attenuated Sindbis virus (21) and used at titers to achieve ~90% infection for biochemistry experiments and ~20% for confocal imaging to allow visualization of individual neurons.

Cell Line Culture—HEK293T cells were maintained in Dulbecco's modified Eagle's medium (Invitrogen) supplemented with 4.5 g/liter glucose, 10% fetal bovine serum, and penicillin/streptomycin. Cells were transfected with TransIt (Cambridge Bioscience). Typically, 1 μ g of each plasmid was used, and cells were lysed and assayed after 48 h. Cells were lysed in buffer containing 150 mM NaCl, 25 mM HEPES, 1% Triton X-100, and 0.1% SDS (pH 7.4). *N*-Ethylmaleimide was used at 20 mM during cell lysis.

Electrophysiology—Parasagittal hippocampal slices 300–400 μ m thick were prepared as described previously (7) in accordance with Home Office guidelines. Slices were allowed to recover for 60 min at 37 °C in culture medium \pm 1 μ M TTX. Sindbis virus was microinjected into the CA1 pyramidal cell layer, and recordings from both TTX- and non-TTX-treated slices were made after 24 h. Submerged slices were perfused with artificial cerebrospinal fluid + 50 μ M picrotoxin at room temperature. Virus-infected neurons were identified by GFP fluorescence, and whole-cell recordings of excitatory postsynaptic currents (EPSCs) were collected first from an infected neuron and subsequently from a neighboring non-infected neuron using the same stimulus intensity and position. Stimulus intensity was adjusted to give an EPSC amplitude of ~50 pA in the infected cell. This explains why the AMPA responses in non-infected neurons in *panel B* of Fig. 3 are larger than in *panels A, D, and E*. Cells were voltage-clamped at -70 mV, and synaptic responses were evoked with 100- μ s square voltage steps applied at 0.1 Hz through bipolar stimulating electrodes (FHC, Inc.) located in the stratum radiatum. For determination of the rectification index, isolated AMPAR-mediated responses were recorded at -70 , 0, and $+40$ mV in the presence of D-AP5 (100 μ M). The rectification index was calculated as the ratio of the *I/V* plot slopes between -70 and 0 mV and between 0 and

$+40$ mV data. Paired or unpaired Student's *t* tests were used as appropriate.

Surface Biotinylation and Western Blotting—Surface biotinylation using sulfo-NHS-SS-biotin (Pierce) was performed as described previously (22). Typically, 75 μ g of Triton X-100-solubilized protein was incubated with 20 μ l of streptavidin-agarose in a total volume of 500 μ l for 2 h at 4 °C. Surface fractions were resolved by SDS-PAGE and subjected to Western blotting with anti-GluA1 or anti-GluA2 antibody (23). Antibodies were from the indicated manufacturers: monoclonal anti-GluA1 and anti-GluA2 (Millipore), monoclonal anti-Arc/Arg3.1 and anti-SUMO-1 (D11, Santa Cruz Biotechnology; or clone 21C7, Developmental Studies Hybridoma Bank, University of Iowa), polyclonal anti-SUMO-2 and anti-SENP3 (Cell Signaling), polyclonal anti-SENP1 (Imgenex), and monoclonal β -tubulin (Sigma-Aldrich). Western blots were quantified using NIH ImageJ or LI-COR Image Studio software. For surface expression assays, surface levels of GluA1/2 were normalized to total GluA1/2 levels. Arc and SENP1/3 levels were normalized to β -tubulin levels.

Immunoprecipitation of SUMOylated Arc—Adult rat brains were homogenized in binding buffer (150 mM NaCl and 25 mM HEPES (pH 7.4)) with protease inhibitors (1 \times Complete, Roche Applied Science) either with or without 20 mM *N*-ethylmaleimide and centrifuged at 1500 $\times g$ for 10 min to pellet cell debris and nuclei. The supernatant was solubilized for 1 h at 4 °C in 1% Triton X-100, and insoluble matter was removed by centrifugation at 15,000 $\times g$ for 10 min. 1 ml of this lysate (~5 mg of total protein) was incubated with protein A-Sepharose beads, 10 μ g of anti-Arc antibody (clone H-6, Santa Cruz Biotechnology), and binding buffer to make the final detergent concentration 0.25%. The reaction was incubated at 4 °C for 2 h, after which the beads were washed three times. After washing, bound protein was eluted from the beads using SDS sample buffer and resolved by SDS-PAGE.

Bacterial SUMOylation Assay—The bacterial SUMOylation assay was performed as described previously (24). Briefly, full-length rat Arc was cloned into the pGEX4T-1 vector. This and a plasmid expressing E1, E2, and SUMO-1 were transformed into *Escherichia coli* BL21 for protein expression. Bacterial cultures were grown to $A_{600} \sim 1.0$ before induction of protein expression with 0.25 mM isopropyl β -D-thiogalactopyranoside and incubated overnight at 18 °C. Cultures were pelleted and lysed by sonication in binding buffer with protease inhibitors, and GST-Arc was purified on glutathione-Sepharose. Before elution, half of the glutathione-Sepharose was treated with 20 nM recombinant SENP1 for 1 h at room temperature. Beads were washed, and proteins were eluted with Laemmli buffer, resolved by SDS-PAGE, and Western-blotted for SUMO-1 and Arc.

Immunocytochemistry and Confocal Microscopy—Hippocampal neurons were treated with 1 μ M TTX for 24 h and then fixed for 5 min with 4% paraformaldehyde in PBS. Surface AMPARs were labeled with primary antibody against the N terminus of rat GluA1 (Calbiochem) and Cy3-conjugated secondary antibody (1:500) under non-permeant conditions. Neurons were then fixed for 12 min with 4% paraformaldehyde, permeabilized with digitonin (10 min; Sigma D141), incubated

with 10% horse serum (20 min), and incubated with mouse monoclonal anti-SUMO-1 antibody (clone 21C7; 1:100). Neurons were labeled with Cy5-conjugated anti-mouse antibody (1:500). Confocal images were acquired with a Zeiss LSM 510 confocal microscope. *z*-stacks of 5–10 images were taken at 1024 × 1024 resolution with *z*-step of 0.5 μm. Images for all conditions in a particular experiment were obtained using identical acquisition parameters and were analyzed using NIH ImageJ software. Neurons were selected blindly based on GFP fluorescence. Quantification of GluA1 and SUMO-1 intensities was carried out by thresholding the enhanced GFP or fluorescence signal in ImageJ to define outlines of neurons, and the average fluorescence within this area was calculated. At least 10 neurons and three to five regions of interest for each condition from three independent experiments were analyzed. Data are expressed as means ± S.E., and significance was determined using two-tailed *t* tests. Values were then normalized to untreated control cells. For presentation, images were processed using Adobe Photoshop software by adjusting the brightness and contrast levels to the same degree for all conditions illustrated in each experiment.

RESULTS AND DISCUSSION

We used 1 μM TTX for 24 h to suppress synaptic activity in cortical neuronal cultures at 21 days *in vitro* (25), and as expected, we detected robust increases in GluA1 and GluA2 surface expression using surface biotinylation (Fig. 1A). We also observed parallel increases in levels of protein conjugation by SUMO-1, but not SUMO-2/3 (Fig. 1B). These Western blots are samples of all SUMO-1- or SUMO-2/3-conjugated proteins, but because SUMOylation patterns vary considerably between different sets of neurons, the entire lane was quantified rather than individual bands. Because a likely mechanism for increased SUMO-1-ylation is decreased deSUMOylation, we assessed the levels of the broad-specificity SUMO-specific protease SENP1. SENP1 was significantly decreased in lysates of TTX-treated neurons (Fig. 1C), consistent with decreased synaptic activity increasing the stability of protein SUMO-1-ylation via down-regulation of SENP1. In contrast, the levels of SENP3, which displays specificity for SUMO-2/3-ylation (26), were significantly increased following TTX treatment (Fig. 1C). Thus, these differential changes in SENP enzymes that have different SUMO paralogue specificities can account for the selective increase in protein conjugation by SUMO-1 following blockade of synaptic activity.

To determine whether this decrease in SENP1 and the consequent increase in the stability of protein SUMOylation play a role in the increase in AMPAR surface expression, we virally overexpressed the catalytic domain (residues 351–644) of SENP1 (hereafter referred to as SENP1(active)) or the same construct with an active site mutation rendering it catalytically inactive (SENP1(C603S)). SENP1(active), but not SENP1(C603S), reduces total neuronal SUMOylation levels in neurons (27). In non-infected neurons and neurons expressing inactive SENP1(C603S), TTX caused a significant increase in surface GluA1. In neurons expressing SENP1(active), however, there was no TTX-induced increase in surface GluA1 (Fig. 1D). Importantly, overexpression of the catalytic domain of SENP1

had no effect on GluA1 surface expression in the absence of TTX (Fig. 1E). Interestingly, infection of neurons with a virus expressing SUMO-1 and Ubc9, which increased cellular SUMOylation (supplemental Fig. S1), caused a significant increase in surface GluA1, implying that increases in cellular SUMOylation are sufficient to drive increases in GluA1 surface trafficking.

The effects of SENP1(active) and SENP1(C603S) on surface GluA1 and total SUMO-1 levels in individual hippocampal neurons were assessed by confocal microscopy. SUMO-1 and surface GluA1 both increased in TTX-treated cells (Fig. 2, A and B). In agreement with our biochemical data, overexpression of SENP1(active) significantly decreased dendritic SUMO-1 levels but had no effect on surface GluA1 in control non-TTX-treated neurons (Fig. 2m C–E). However, in TTX-treated neurons, SENP1(active) overexpression significantly reduced the TTX-induced increase in surface GluA1 and in SUMOylation compared with expression of inactive SENP1(C603S) (Fig. 2, C, D, F, and G). We note that, unlike for the experiments in Fig. 1, SENP1 infection did not completely prevent the TTX-induced increase in surface expression. This may be attributable to the different experimental techniques, the density of neurons or the types of neurons, high-density cortical cells for biochemistry in Fig. 1, and low-density hippocampal cells for imaging in Fig. 2. Nonetheless, the decrease in the TTX effect shown in Fig. 2F is significant and corresponds to the decrease in TTX-induced SUMOylation observed in Fig. 2G in SENP1(active)-infected cells, consistent with these two effects being linked.

These results indicate that protein SUMOylation is required for the increase in GluA1 surface expression following sustained inhibition of synaptic activity. To confirm that the increase in surface GluA1 corresponds to a functional change, we next tested the effects of SENP1(active) expression on AMPAR-mediated EPSCs at Schaffer collateral synapses on CA1 pyramidal neurons in the CA1 region of cultured hippocampal slices. Slices were infected with Sindbis virus expressing GFP-tagged SENP1(active) or SENP1(C603S) and incubated for 24 h in the absence or presence of TTX to induce synaptic scaling. Infected neurons were identified by GFP fluorescence, and EPSCs were recorded from the infected and vicinal non-infected cells from the same slice.

SENP1(active) overexpression had no effect on control non-TTX-treated neurons (59.1 ± 9.8 versus 56.1 ± 12.7 pA for infected versus non-infected, respectively ($n = 7$); $p > 0.05$) (Fig. 3, A and C). Similarly, overexpression of SENP1(C603S) had no effect on EPSCs in either TTX- or non-TTX-untreated neurons (65.2 ± 11.8 versus 59.5 ± 15.4 pA ($n = 7$); $p > 0.05$) (Fig. 3, D–F). However, overexpression of SENP1(active) reduced EPSCs in TTX-treated cells compared with control non-infected neurons (43.2 ± 4.6 versus 104.8 ± 21.2 pA for infected versus non-infected, respectively ($n = 9$); $p < 0.05$) (Fig. 3, B and C). These results agree with our data from Figs. 1 and 2, showing that SENP1(active) overexpression affects only TTX-induced increases in surface GluA1 rather than constitutive surface expression/recycling. It should be noted that, in these experiments, the stimulus intensity was adjusted to give an EPSC amplitude of ~50 pA in the infected cell, so responses

Synaptic Scaling and SUMOylation

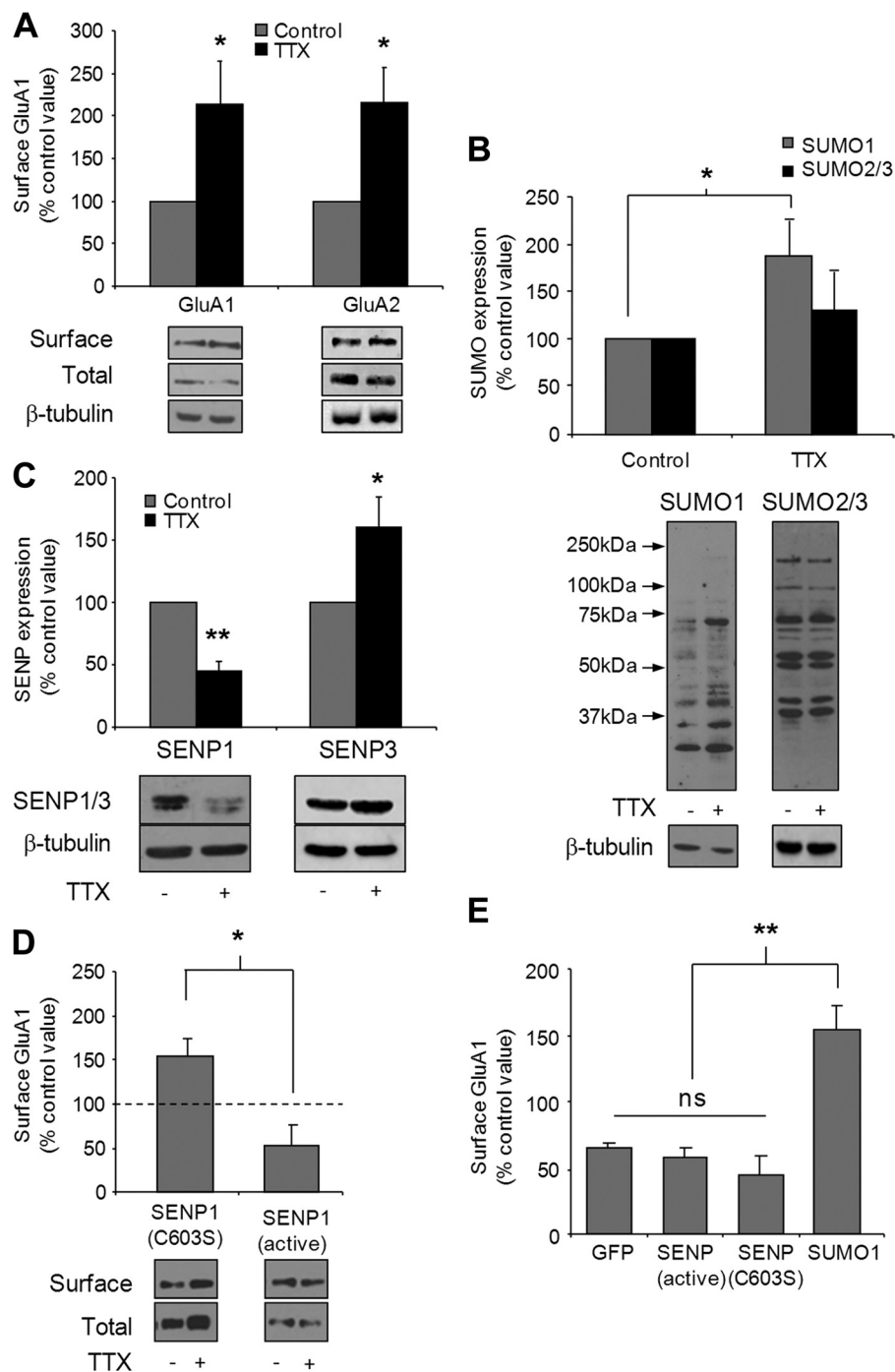


FIGURE 1. Synaptic scaling decreases SENP1 and increases SUMO-1 conjugation. *A*, a 24-h treatment with 1 μ M TTX increased surface expression of GluA1 and GluA2 in cortical neurons. Surface GluA1/2 was normalized to total GluA1/2. Data are the means \pm S.E. of four experiments. *B*, quantification of SUMO conjugation after a 24-h treatment with 1 μ M TTX and representative SUMO-1 and SUMO-2/3 blots. The total levels of SUMO-1 or SUMO-2/3 (the entire lane) were normalized to the levels of β -tubulin ($n = 3$). *C*, quantification and representative blots of SENP1 and SENP3 normalized to β -tubulin levels with and without TTX treatment ($n = 6$ for SENP1, and $n = 3$ for SENP3). *D*, overexpression of SENP1(active) prevented TTX-induced synaptic scaling. GluA1 after TTX treatment was normalized to total GluA1 levels and is expressed as a percentage of the control value, represented by the dashed line ($n = 4$). *E*, SENP1(active) or SENP1(C603S) overexpression did not alter surface expression of GluA1, but SUMO-1/Ubc9 overexpression did ($n = 4$). *, $p < 0.05$; **, $p < 0.01$ (Student's *t* test); ns, not significant.

in non-infected neurons in *panel B* in Fig. 3 are larger than those in *panels A, D*, and *E*. Thus, SENP1(active) reverses protein SUMOylation and thereby prevents the TTX-evoked increase in AMPAR EPSCs. We also tested if overexpression of SENP1(active) altered the ratio of GluA1 and GluA2. AMPAR-mediated EPSCs were isolated by bath application of D-AP5

(100 μ M), and the rectification index was determined by recording EPSCs at -70 , 0 , and $+40$ mV. Consistent with previous reports that rectification does not change in scaling (2, 28), we observed no changes in rectification with SENP1(active) or SENP1(C603S) (supplemental Fig. S2). These results indicate that SUMOylation does not alter AMPAR subunit stoichiometry.

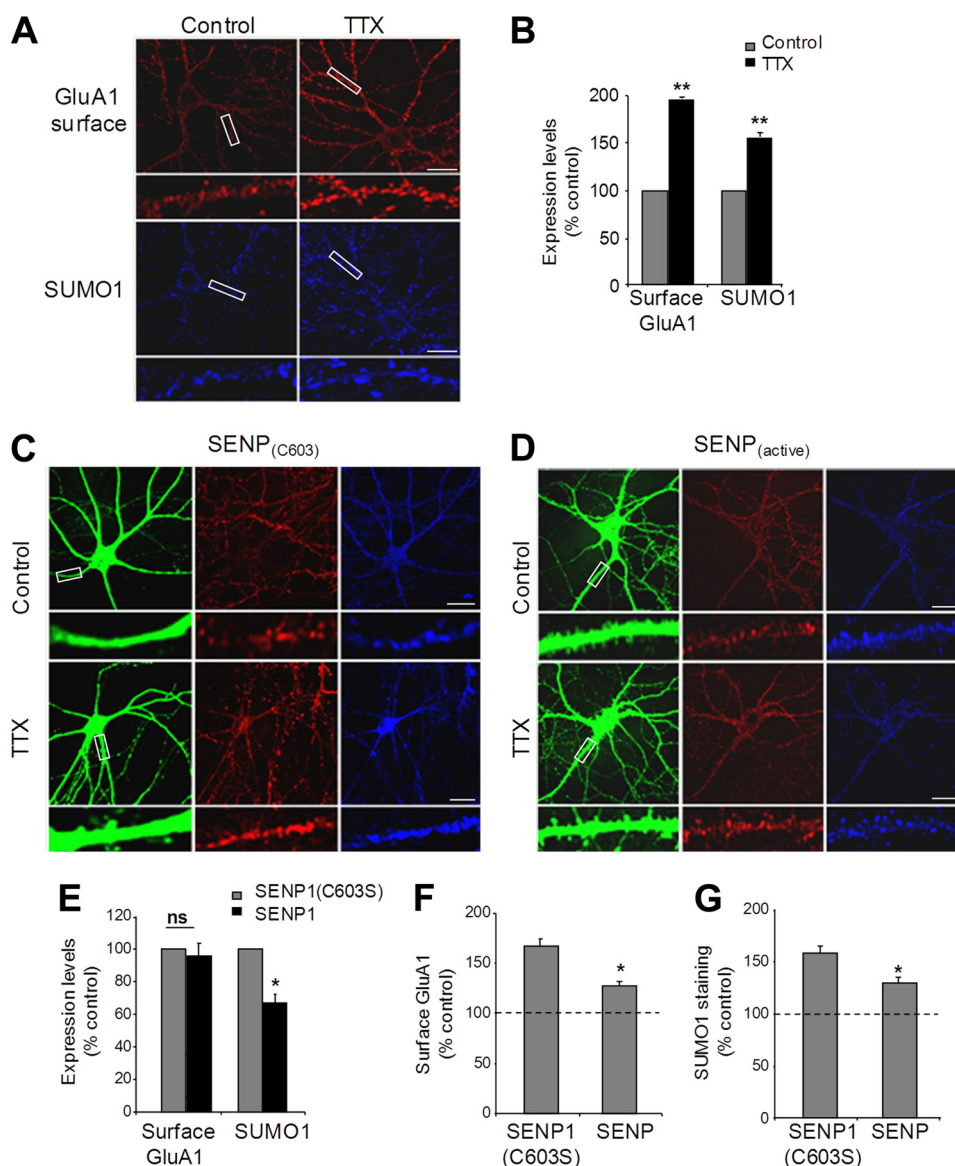


FIGURE 2. TTX increases surface expression of GluA1 and expression of SUMO-1. *A*, control and 24-h TTX ($1 \mu\text{M}$)-treated cultured hippocampal neurons showing regions of interest used for quantification of expression levels. Enlarged regions of interest are indicated by boxes. *Scale bars* = $20 \mu\text{m}$. *B*, quantification of surface expression of GluA1 and total SUMO-1, expressed as a percentage of control non-TTX-treated cells ($n = 3$, *i.e.* three separate experiments, each assaying three to five regions of interest in 10 different cells). *C* and *D*, SENP1(C603S)- and SENP1(active)-overexpressing cells, respectively. *E*, effects of SENP1(active) overexpression on SUMO-1 and surface GluA1 in neurons without TTX treatment. Surface GluA1 is expressed as a percentage of control cells expressing SENP1(C603S) ($n = 3$, as described above). *F*, surface GluA1 in cells treated with TTX expressing either SENP1(C603S) or SENP1(active) is expressed as a percentage of surface GluA1 in cells without TTX treatment ($n = 3$, as described above). *G*, SUMO-1 levels in cells treated with TTX and infected with either SENP1(C603S) or SENP1(active) virus are expressed as a percentage of SUMO-1 levels in cells without TTX treatment ($n = 3$, as described above). *, $p < 0.05$; *ns*, not significant. **, $p < 0.01$.

Arc plays a key role in scaling, and it has been suggested to be a SUMO substrate (20). We therefore investigated whether SUMOylation could regulate scaling by altering Arc stability using wild-type Arc (Arc-WT) and Arc- ΔKK , a mutant in which the two high-probability SUMOylation lysines (Lys-110 and Lys-268) were mutated to alanines. In HEK293T cells transfected with Arc-WT, a 75-kDa band was detected in addition to the ~ 50 -kDa Arc band (Fig. 4A). This band was more intense when Arc was coexpressed with the SUMO-conjugating enzyme Ubc9 but was completely absent in the Arc- ΔKK mutant. Ubc9 coexpression would be expected to increase the SUMO conjugation of any cellular SUMO targets, suggesting that this band is SUMOylated Arc. Note that although SUMO-1

is 10 kDa, SUMOylation usually results in a larger apparent molecular mass shift due to the branched nature of SUMOylated protein. These results indicate that Arc is indeed a SUMO substrate and demonstrate that Arc- ΔKK is a SUMO-deficient mutant. A similar endogenous 75-kDa SUMO-reactive band was also immunoprecipitated from rat brain lysate using monoclonal anti-Arc antibody (Fig. 4B). Consistent with it being SUMO-Arc, the band was reduced when *N*-ethylmaleimide, a cysteine protease inhibitor, was omitted during preparation of the brain lysate. A second higher molecular mass band at ~ 120 kDa was also immunoprecipitated, suggesting that Arc may be modified by more than one SUMO in neurons. Taken together, these data indicate that Arc can be

Synaptic Scaling and SUMOylation

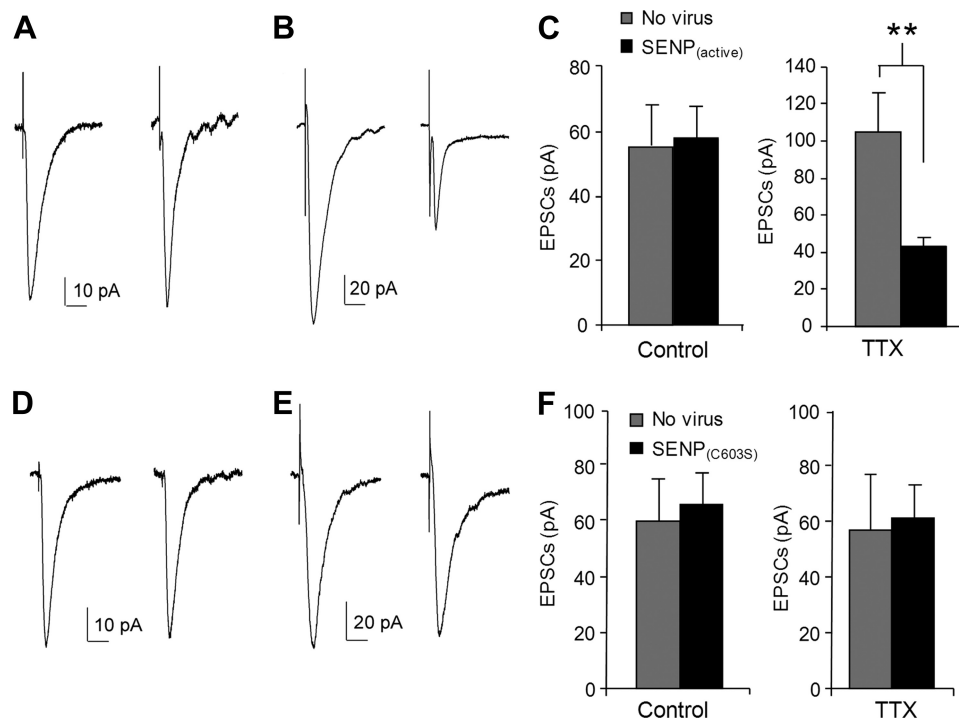


FIGURE 3. SENP1(active) expression reduces AMPAR-mediated EPSCs in TTX-treated neurons. *A*, AMPAR EPSCs recorded from the non-infected (*left*) and SENP1(active)-infected (*right*) control (untreated) hippocampal slices. *B*, AMPAR EPSCs recorded from the non-infected (*left*) and SENP1(active)-infected (*right*) slices treated with TTX. *C*, average values of AMPA EPSCs for control (gray bars) and SENP1(active)-infected (black bars) cells in control slices (*left*; $n = 7$) and in slices treated with TTX (*right*; $n = 9$). **, $p < 0.01$. *D*, AMPAR EPSCs recorded from the non-infected (*left*) and SENP1(C603S)-infected (*right*) control (untreated) hippocampal slices. *E*, AMPAR EPSCs recorded from the non-infected (*left*) and SENP1(C603S)-infected (*right*) slices treated with TTX. *F*, average values of AMPA EPSCs for control (gray bars) and SENP1(C603S)-infected (black bars) cells in control slices (*left*; $n = 7$) and in slices treated with TTX (*right*; $n = 7$). The time scale was 40 ms in all traces.

SUMOylated *in vivo* and that Lys-110 and Lys-268 are the likely SUMO sites.

To provide further evidence that Arc is directly conjugated by SUMO-1 and deSUMOylated by SENP1, we performed a bacterial SUMOylation assay with GST-tagged Arc. As bacteria have no SUMOylation machinery, this is a tightly controlled system. We purified SUMOylated GST-Arc from the bacterial lysate (Fig. 4C) as shown by a higher molecular mass SUMO- and Arc-reactive band above the ~75-kDa band for GST-Arc. Furthermore, this band was completely removed by a 1 h treatment with recombinant SENP1, demonstrating that Arc is deSUMOylated by SENP1.

We next expressed GFP-Arc or GFP-Arc- Δ KK in neurons. Arc-WT and Arc- Δ KK levels were reduced by ~60% after a 24-h TTX treatment (Fig. 4D), suggesting that SUMOylation does not affect Arc degradation. To determine whether SUMOylation alters Arc function, we expressed GFP-Arc or GFP-Arc- Δ KK and assessed GluA1 surface expression after a 24-h TTX treatment (Fig. 4E). Under basal conditions, both Arc-WT and Arc- Δ KK reduced GluA1 surface expression (Fig. 4, E and F), indicating that the Δ KK mutation does not affect the ability of Arc to endocytose GluA1.

Consistent with Arc SUMOylation being involved in scaling, overexpression of Arc- Δ KK prevented the TTX-induced increase in AMPAR surface expression (Fig. 4, E and G). Surprisingly, however, overexpression of Arc-WT caused a greater reduction in surface GluA1 in TTX-treated neurons than in control neurons. Interestingly, this effect has been observed, but not discussed, previously (16).

Possible explanations are that overexpression of Arc-WT interferes with other synaptic processes such as cytoskeletal remodeling or that Arc-WT might chelate SUMO-1 and reduce SUMOylation of other targets necessary for maintaining GluA1 surface expression. Arc overexpression could also disrupt the balance between AMPAR exocytosis, membrane retention, and endocytosis. More specifically, reduced network activity resets synaptic AMPAR trafficking and recycling to ensure that more AMPARs are present at synapses. This can be mediated by reduced endocytosis, increased rates of *de novo* exocytosis, and/or reduced recycling and thus increased residence time at the plasma membrane. We hypothesize that, under these reset parameters, overexpression of Arc increases endocytosis, but the equilibrium is perturbed, and there is no accompanying increase in recycling, resulting in a net decrease in surface GluA1 below that observed in non-TTX-treated cells. Importantly, our data indicate an activity-dependent rather than a constitutive role for protein SUMOylation in AMPAR trafficking, consistent with no effect of SENP1(active) on surface AMPAR in the absence of TTX. This activity dependence likely accounts for the previously reported lack of effect of infusion of SUMO-1 or SENP1 on basal AMPAR EPSCs in hippocampal neurons (7).

In good correlation with our results for SENP1(active) overexpression, the effects of Arc- Δ KK differed from those of Arc-WT only after TTX pretreatment. Specifically, in neurons expressing Arc- Δ KK, there was no difference between TTX- and non-TTX-treated cells. These results are consistent with the hypothesis that Arc SUMOylation is a requirement for the

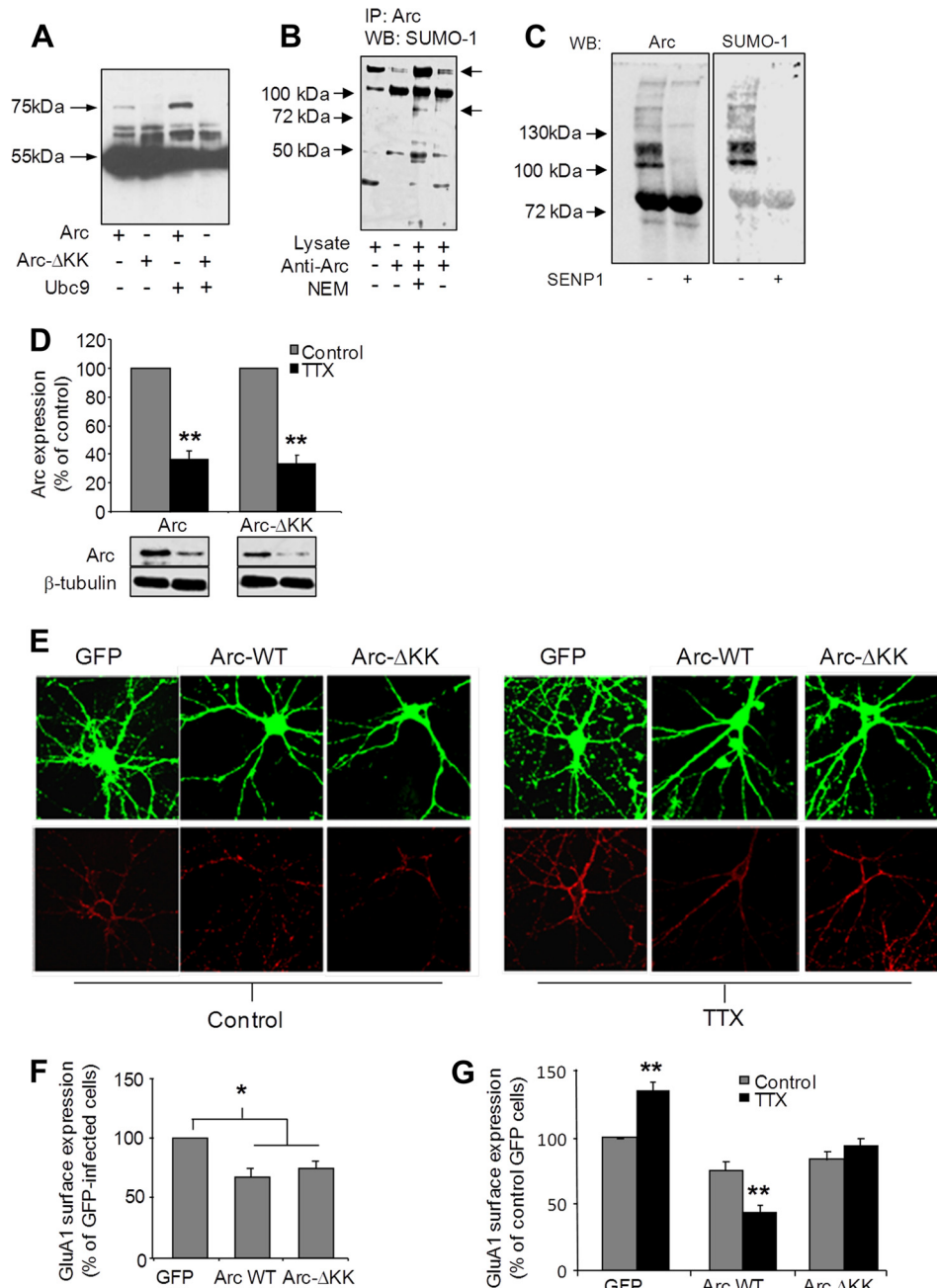


FIGURE 4. Arc SUMOylation is required for synaptic scaling. *A*, Arc was SUMOylated in HEK293T cells at Lys-110 and Lys-268. Shown is a Western blot for Arc in HEK293T lysates from cells transfected with either Arc or Arc-ΔKK (K110A/K268A mutant) with or without Ubc9. *B*, immunoprecipitation of SUMO-Arc from rat brain lysate in the absence and presence of *N*-ethylmaleimide. Immunoprecipitation (IP) was performed with anti-Arc antibody (clone H-6), and Western blotting (WB) was performed with anti-SUMO-1 antibody (clone 21C7). *C*, bacterial SUMOylation assay of Arc. GST-Arc from bacteria expressing SUMOylation machinery (E1, E2, and SUMO-1) was purified on glutathione-Sepharose, and half was treated with 20 nM recombinant SENP1 for 1 h at room temperature. Eluates from glutathione-Sepharose were blotted for Arc and SUMO-1. *D*, overexpressed Arc-ΔKK displayed the same response to TTX as Arc-WT in neurons treated for 24 h with 1 μM TTX. The levels of Arc were normalized to tubulin levels ($n = 6$). *E*, representative immunostaining of non-TTX- and TTX-treated hippocampal neurons infected with the GFP control, GFP-Arc-WT, or GFP-Arc-ΔKK Sindbis virus. Images are shown of GFP and surface GluA1 (red) fluorescence for each neuron. *F*, quantification of GluA1 surface expression in cells without TTX treatment, expressed as a percentage of surface expression in GFP-infected cells ($n = 4$, each repeat assaying 10 neurons). *G*, quantification of GluA1 surface expression after a 24-h treatment with 1 μM TTX in cells infected with viruses, expressed as a percentage of surface expression in GFP-infected cells without TTX ($n = 4$, as described above). *, $p < 0.05$; **, $p < 0.01$ (Student's *t* test).

forward trafficking of GluA1 to the cell surface during chronic activity blockade to express homeostatic plasticity. Given the complexity and multilayered control of AMPAR trafficking, we consider it likely that other, as yet unidentified SUMO target proteins also play important roles in the modulation of AMPAR trafficking.

In summary, our results demonstrate that decreased SENP1 is permissive for synaptic scaling and suggest that SUMOylation of Arc is a key arbiter of homeostatic plasticity. This represents a previously unsuspected regulatory mechanism for the control of long-term responsiveness of neurons to changes in network activity.

REFERENCES

- Henley, J. M., Barker, E. A., and Glebov, O. O. (2011) Routes, destinations, and delays: recent advances in AMPA receptor trafficking. *Trends Neurosci.* **34**, 258–268
- Turrigiano, G. G. (2008) The self-tuning neuron: synaptic scaling of excitatory synapses. *Cell* **135**, 422–435
- Pozo, K., and Goda, Y. (2010) Unraveling mechanisms of homeostatic synaptic plasticity. *Neuron* **66**, 337–351
- Wilkinson, K. A., and Henley, J. M. (2010) Mechanisms, regulation, and consequences of protein SUMOylation. *Biochem. J.* **428**, 133–145
- Martin, S., Wilkinson, K. A., Nishimune, A., and Henley, J. M. (2007) Emerging extranuclear roles of protein SUMOylation in neuronal function and dysfunction. *Nat. Rev. Neurosci.* **8**, 948–959
- Wilkinson, K. A., Nakamura, Y., and Henley, J. M. (2010) Targets and consequences of protein SUMOylation in neurons. *Brain Res. Rev.* **64**, 195–212
- Martin, S., Nishimune, A., Mellor, J. R., and Henley, J. M. (2007) SUMOylation regulates kainate receptor-mediated synaptic transmission. *Nature* **447**, 321–325
- Konopacki, F. A., Jaafari, N., Rocca, D. L., Wilkinson, K. A., Chamberlain, S., Rubin, P., Kantamneni, S., Mellor, J. R., and Henley, J. M. (2011) Agonist-induced PKC phosphorylation regulates GluK2 SUMOylation and kainate receptor endocytosis. *Proc. Natl. Acad. Sci. U.S.A.* **108**, 19772–19777
- Chao, H. W., Hong, C. J., Huang, T. N., Lin, Y. L., and Hsueh, Y. P. (2008) SUMOylation of the MAGUK protein CASK regulates dendritic spineogenesis. *J. Cell Biol.* **182**, 141–155
- Shalizi, A., Bilimoria, P. M., Stegmüller, J., Gaudillière, B., Yang, Y., Shuai, K., and Bonni, A. (2007) PIASx is a MEF2 SUMO E3 ligase that promotes postsynaptic dendritic morphogenesis. *J. Neurosci.* **27**, 10037–10046
- Shalizi, A., Gaudillière, B., Yuan, Z., Stegmüller, J., Shirogane, T., Ge, Q., Tan, Y., Schulman, B., Harper, J. W., and Bonni, A. (2006) A calcium-regulated MEF2 sumoylation switch controls postsynaptic differentiation. *Science* **311**, 1012–1017
- Feligioni, M., Nishimune, A., and Henley, J. M. (2009) Protein SUMOylation modulates calcium influx and glutamate release from presynaptic terminals. *Eur. J. Neurosci.* **29**, 1348–1356
- Plant, L. D., Dowdell, E. J., Dementieva, I. S., Marks, J. D., and Goldstein, S. A. (2011) SUMO modification of cell surface Kv2.1 potassium channels regulates the activity of rat hippocampal neurons. *J. Gen. Physiol.* **137**, 441–454
- Bramham, C. R., Worley, P. F., Moore, M. J., and Guzowski, J. F. (2008) The immediate-early gene *arc/arg3.1*: regulation, mechanisms, and function. *J. Neurosci.* **28**, 11760–11767
- Greer, P. L., Hanayama, R., Bloodgood, B. L., Mardinly, A. R., Lipton, D. M., Flavell, S. W., Kim, T. K., Griffith, E. C., Waldon, Z., Maehr, R., Ploegh, H. L., Chowdhury, S., Worley, P. F., Steen, J., and Greenberg, M. E. (2010) The Angelman syndrome protein Ube3A regulates synapse development by ubiquitinating Arc. *Cell* **140**, 704–716
- Shepherd, J. D., Rumbaugh, G., Wu, J., Chowdhury, S., Plath, N., Kuhl, D., Hugarir, R. L., and Worley, P. F. (2006) Arc/Arg3.1 mediates homeostatic synaptic scaling of AMPA receptors. *Neuron* **52**, 475–484
- Chowdhury, S., Shepherd, J. D., Okuno, H., Lyford, G., Petralia, R. S., Plath, N., Kuhl, D., Hugarir, R. L., and Worley, P. F. (2006) Arc/Arg3.1 interacts with the endocytic machinery to regulate AMPA receptor trafficking. *Neuron* **52**, 445–459
- Shepherd, J. D., and Bear, M. F. (2011) New views of Arc, a master regulator of synaptic plasticity. *Nat. Neurosci.* **14**, 279–284
- Béique, J. C., Na, Y., Kuhl, D., Worley, P. F., and Hugarir, R. L. (2011) Arc-dependent synapse-specific homeostatic plasticity. *Proc. Natl. Acad. Sci. U.S.A.* **108**, 816–821
- Bramham, C. R., Alme, M. N., Bittins, M., Kuipers, S. D., Nair, R. R., Pai, B., Panja, D., Schubert, M., Soule, J., Tiron, A., and Wibrand, K. (2010) The Arc of synaptic memory. *Exp. Brain Res.* **200**, 125–140
- Kantamneni, S., Wilkinson, K. A., Jaafari, N., Ashikaga, E., Rocca, D., Rubin, P., Jacobs, S. C., Nishimune, A., and Henley, J. M. (2011) Activity-dependent SUMOylation of the brain-specific scaffolding protein GISP. *Biochem. Biophys. Res. Commun.* **409**, 657–662
- Kantamneni, S., Corrêa, S. A., Hodgkinson, G. K., Meyer, G., Vinh, N. N., Henley, J. M., and Nishimune, A. (2007) GISP: a novel brain-specific protein that promotes surface expression and function of GABA_B receptors. *J. Neurochem.* **100**, 1003–1017
- Feligioni, M., Holman, D., Haglerod, C., Davanger, S., and Henley, J. M. (2006) Ultrastructural localization and differential agonist-induced regulation of AMPA and kainate receptors present at the presynaptic active zone and postsynaptic density. *J. Neurochem.* **99**, 549–560
- Wilkinson, K. A., Nishimune, A., and Henley, J. M. (2008) Analysis of SUMO-1 modification of neuronal proteins containing consensus SUMOylation motifs. *Neurosci. Lett.* **436**, 239–244
- Sutton, M. A., Ito, H. T., Cressy, P., Kempf, C., Woo, J. C., and Schuman, E. M. (2006) Miniature neurotransmission stabilizes synaptic function via tonic suppression of local dendritic protein synthesis. *Cell* **125**, 785–799
- Gong, L., and Yeh, E. T. (2006) Characterization of a family of nucleolar SUMO-specific proteases with preference for SUMO-2 or SUMO-3. *J. Biol. Chem.* **281**, 15869–15877
- Cimarosti, H., Ashikaga, E., Jaafari, N., Dearden, L., Rubin, P., Wilkinson, K. A., and Henley, J. M. (2011) Enhanced SUMOylation and SENP1 protein levels following oxygen and glucose deprivation in neurones. *J. Cereb. Blood Flow Metab.* **32**, 17–22
- Wierenga, C. J., Ibata, K., and Turrigiano, G. G. (2005) Postsynaptic expression of homeostatic plasticity at neocortical synapse. *J. Neurosci.* **25**, 2895–2905